Hindawi
International Journal of Chemical Engineering
Volume 2022, Article ID 1891419, 11 pages
https://doi.org/10.1155/2022/1891419

Research Article

Studies on Corrosion Behavior of Mg-Al-Zn-RE Cast Alloy with Powder-Coated Al and CED Mg by Salt Spray Test, Immersion Test, and Electrochemical Test

R. Krishnan,[1] S. Manivannan,[2] Praveen Bhai Patel,[3] Pravin P Patil,[4] R. Venkatesh,[5] Natrayan L,[5] and Subash Thanappan[6]

[1]*Department of Mechanical Engineering, Karpagam Academy of Higher Education, Coimbatore, Tamil Nadu, India*
[2]*Centre for Material Science, Department of Mechanical Engineering, Karpagam Academy of Higher Education, Coimbatore, Tamil Nadu, India*
[3]*Department of Chemical Engineering, University Institute of Engineering and Technology, C S J M University, Kanpur, India*
[4]*Department of Mechanical Engineering, Graphic Era Deemed to be University, Bell Road, Clement Town 248002, Dehradun, Uttarakhand, India*
[5]*Department of Mechanical Engineering, Saveetha School of Engineering, SIMATS, Chennai, Tamil Nadu 602105, India*
[6]*Department of Civil Engineering, Ambo University, Ambo, Ethiopia*

Correspondence should be addressed to S. Manivannan; manivannan.s@kahedu.edu.in and Subash Thanappan; thanappansubash@gmail.com

Received 22 May 2022; Revised 23 June 2022; Accepted 28 June 2022; Published 13 July 2022

Academic Editor: G.L. Balaji

Cathodic electrodeposition (CED) was used to coat the cast magnesium alloy Mg-9Al-1Zn-xRE with aluminum powder and epoxy. Immersion and salt spray tests (ASTM B117) at room temperature for a total of 240 hours have been performed to assess the corrosion performances of AZ91D magnesium alloy. At each 24-hour interval, the samples were checked for any damage or deterioration of the coating surface morphology. The X-ray diffraction (XRD) analysis confirmed the phases, and scanning electron microscopy (SEM) with EDS analysis confirmed the phase composition. The electrochemical results show that CED epoxy coatings have superior adhesiveness and corrosion resistance compared to powder-coated aluminum and cast magnesium. The salt spray and immersion test results also confirm that CED epoxy coating exhibits good corrosion resistance.

1. Introduction

Modern concerns include the increased usage of lightweight materials such as Mg, Al, and Ti in constructional applications with the goal of both mass reduction and energy savings [1]. The AZ91D Mg alloy is used in specific application fields such as automobile body construction, marine application, mechanical engineering, and electrical sectors [2]. Furthermore, rising concerns about environmental protection and long-term economic development have heightened interest in lowering greenhouse gas emissions [3]. Because Mg and its alloys exhibit high specific strength compared to other structural metallic materials, they have a wide range of uses due to their high mechanical properties and malleability, damping characteristics, and better shielding on electromagnetic fields [4]. Automobile manufacturers have been studying the bond between the mass of the vehicle and efficiency in fuel for periods so that they can encounter consumer demands for more efficient consumption of fuel [5]. Hence, emissions can be reduced in an era of increasing eco-friendly environment [6]. Magnesium and its alloys are used to replace many parts in various coverings [7]. Magnesium and its alloys, on the other hand, are known to have a hexagonal crystal structure [8]. The alloy displays poor formability due to the formation of numerous slip planes and the consequence of localized slip in the deformed grain boundaries, which causes the formation of built-up stress [9]. Because of its less dense outer layer of MgO and $Mg(OH)_2$,

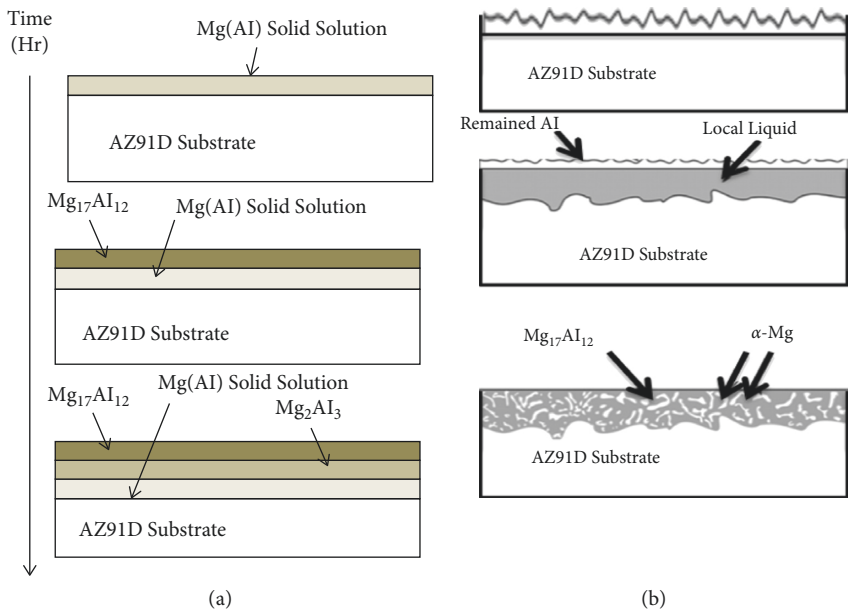

Figure 1: Growth of the surface layers on AZ91D Mg during the coating. (a) Below 437°C and (b) above 437°C.

magnesium and its alloys have poor corrosion [10]. With a 0.81 Pilling-Bed worth ratio, the less dense layer cannot be entirely coated on the entire magnesium surface [11]. It is why Mg and its alloys have poor corrosion resistance at ambient temperature and are unstable when exposed to a high temperature [12]. Physical treatments such as grinding and polishing and chemical treatments such as acidic and alkaline processes are frequently used depending on the need for corrosion-resistant applications [13]. The following requisite preliminary treatment has been used for the organic and inorganic coating processes [14].

2. Different Protective Coatings for Magnesium Alloys (AZ91D)

Mg and its alloys exhibit better physical and mechanical properties, making them ideal for various uses [15]. Its excellent ratio between strength-to-weight makes it ideal for aviation applications. Unfortunately, they are exceedingly corrosive, especially when exposed to salt spray [16]. Epoxy coated on AZ91D substrate kept in contact with the controlled environment to avoid corrosion [17]. In this study, the coating and modification in surface level for improved properties such as corrosion and mechanical strength on magnesium-based substrates are examined in the present research [18]. Magnesium alloy components might not always meet the demand for automotive components in hostile environments [19]. AZ91D alloy's anticorrosion performance is currently a hot topic in the study [20]. The previous research article's findings observed based on the enhancement properties in corrosion performance of AZ alloys utilizing various coating techniques will be the subject of this literature review [21].

2.1. Structure of the Diffusion Coatings. Regardless of the coating method, the presence of an alloy layer is a property of all diffusion coatings shown in Figure 1. The degree of alloying is determined by the coating method. Some of the coatings are formed on the metal substrate that has not been alloyed [22]. The processing parameters such as methods, processing temperature, and processing time (treatment time) have an impact on the microconstituents and elemental composition (phase) of diffusion coatings [23]. The continuous layer of intermetallic compounds formed on the surface after diffusion coatings for Mg was produced at lower temperatures between 200°C and 400°C, regardless of the coating procedure or treatment period [24]. The higher temperature treatment, like 420°C–470°C, produces a two-phase structure enriched in $Mg_{17}Al_{12}$ [25]. The temperatures chosen were 437°C below the eutectic reaction of Mg-Al, based on reaction-diffusion principles [26].

The properties of the AZ91D-coated alloy have received significant attention in this study. Magnesium is a volatile metal with high reactivity. After coating treatment, $Mg_{17}Al_{12}$ or Mg_2Al_3 intermetallic phases are formed on the surfaces, which improved the corrosion resistance of AZ91D alloy. Accelerated methods such as salt spray (ASTM B117 standard) and immersion test (ASTM G14 standard), weight loss, and electrochemical methods can all be utilized (e.g., potentiodynamic tests and electrochemical impedance spectroscopy) to understand the corrosion performances of coated AZ91D magnesium alloys [27]. Before and after coating, the corrosion resistance of AZ91D in Al powders and epoxy has been done with the CED coatings. The uncoated AZ91D, Al powder coating, and CED coating experienced substantial corrosion after being exposed to salt sparing test for less than 12 hours [28]. In aluminium coating specimens, the initial pitting has been observed after increasing the contact duration to more than 72 hours. The weight loss measurement at various temperatures was calculated to understand the corrosion behaviour of Al coating on AZ91D alloy. 3.5wt.% of NaCl solution revealed the Al

Table 1: Composition of AZ91D magnesium alloy.

Aluminum (%)	Zinc (%)	Manganese (%)	Silicon (%)	Iron (%)	Copper (%)	Nickel (%)	Magnesium
9.201	0.90	0.15	0.1	0.005	0.03	0.002	Balance

Table 2: Thickness of coating.

Coating	AZ91D
Powder-coated sample	76 microns
CED-coated sample	78 microns

powder coating and CED Mg coating had significantly higher corrosion resistance than pure Mg [29].

3. Experimental Procedure

In the present investigation, AZ91D magnesium alloy has been selected as the base material. Table 1 presents the chemical composition of AZ91D magnesium alloy, which is confirmed by using optical emission spectroscopy (OES), Test point, Tamil Nadu, India.

3.1. Sample Preparation. Samples for corrosion tests of AZ91D magnesium alloy were cut from rods and machined into the required dimensions [30]. After machining, the final projections were eliminated by emery polishing.

3.2. Macroimages. Table 2 represents the coating thickness of AZ91D magnesium alloy, which confirms that the Al powder coating sample is 76 microns and the Mg CED-coated sample is 78 microns as shown in Figure 2.

3.3. Optical Microscopy. Picral was the etchant used for microstructural investigation. The samples were prepared for examination using optical microscopy. For simple polishing, the cut sample was mounted using a cold setting [31]. The mounted specimens were polished with emery sheets, disc polishing, and diamond paste polishing to achieve a mirror finish. After being etched for 10–15 seconds, the samples were examined under an optical microscope [32]. Microstructures of all samples were photographed at various magnifications to obtain clear information.

3.4. Salt Spraying (ASTM B117) and Immersion Test (ASTM G14). The spraying test, also known as the fog test, is used to determine the rate of corrosion on the coated sample and uncoated samples through the calculation of weight loss methods. It is performed in line with the ASTM B117 standard. The salt spray chamber consists of a fog collector, reservoir, nozzles, and control units, as shown in Figure 3.

The test conditions for the salt spray test are shown in Table 3. According to the ASTM G14 standard, the immersion test is performed and its corrosion rate has been measured on the coated and uncoated samples through the following formula.

The corrosion rate of coated samples was determined using the following formula: the corrosion rate (CR) is equal to 87.6 XW/(DAT) mm/year. W = weight loss in milligrams (mg), D = density of material (g/cm^3), A = area (cm^2), and T = time of exposure (hours).

3.5. Potential-Dynamic Polarization and Impedance Test. The polarization and impedance testing set up is shown in Figure 4. This test provides information about a material's corrosion susceptibility and coating characteristics. The test conditions for the polarization and impedance tests are shown in Table 4.

4. Results and Discussions

The study focuses on creating protective coatings for the AZ91D alloy, enhancing the surface's corrosion resistance. The corrosion rate in sodium chloride solution was determined using a cast sample, a powder-coated sample, and a cathode electrodeposition (CED)-coated epoxy sample [33]. Salt spray, immersion, potential-dynamic polarization, and impedance tests were used to examine the specimens. The samples were taken for metallurgical analysis after testing, and the results were reviewed in terms of how they differed from corrosion tests and how they compared to a cast sample [34]. Figure 5 shows the microstructures for the CED coated by AZ91D+0.1wt.% Ce+0.1wt.% Li Mg alloy and powder coated on AZ91D+0.1wt.%Ce+0.1wt.% Li Mg alloy is characterized by DIC Leica (Leica DM750) optical microscopy [35].

4.1. Microstructure of AZ91D Magnesium Alloy. Figure 6 shows the cross-section micrograph for (a) Al powder coating and (b) epoxy coating on AZ91D+0.1wt.% Ce+0.1wt.% Li Mg alloy. SEM images of epoxy CED samples of AZ91D+0.1wt.% Ce+0.1wt.% Li Mg alloy are shown in Figures 7 and 8. The principal constituent is magnesium, with aluminium and zinc serving as alloying elements. α-Mg and β-$Mg_{17}Al_{12}$ are the main phases found in the microstructure and have been confirmed in the presence of precipitation of beta phases along with the coating areas [36].

4.2. Mechanical Property Studies. Figure 9 shows the mechanical properties, such as tensile test and Vicker's microhardness values, of Al powder coating and epoxy coating on AZ91D samples. Figure 10 shows that Vicker's microhardness measurement was used to determine the microhardness of the coated interfaces by applying the minimum loads [37]. A fixed load of 10 g was applied to a diamond cone for 15–20 seconds at the interfaces. The diamond cone is pressed into the sample's surface, leaving an indentation mark on the sample's surface. The microhardness of the specimen was

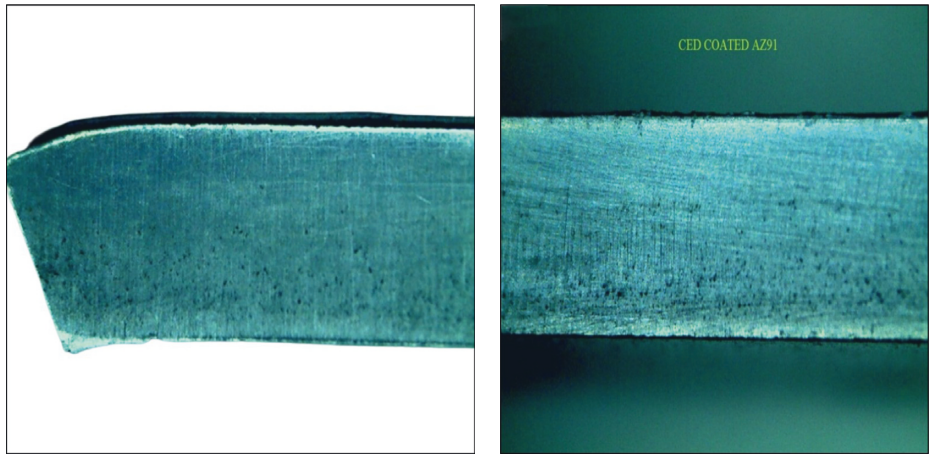

(a) (b)

Figure 2: Macroimages of (a) powder-coated and (b) epoxy CED samples of AZ91D+0.1wt.%Ce+0.1wt.% Li alloy (5X magnification).

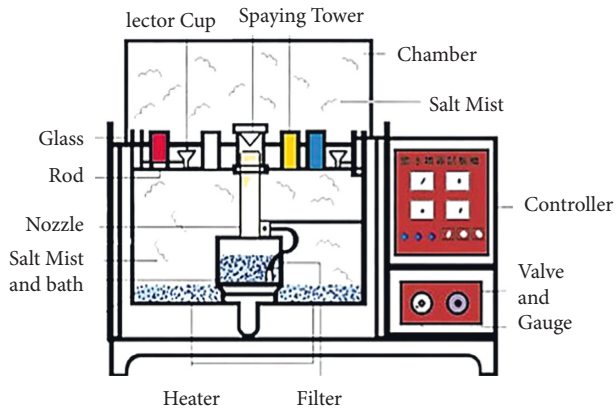

Figure 3: Salt spray testing setup.

Table 3: Conditions for salt spray test.

Temperature	35°C
Pressure	15–25 Psi
pH value	6-7μ

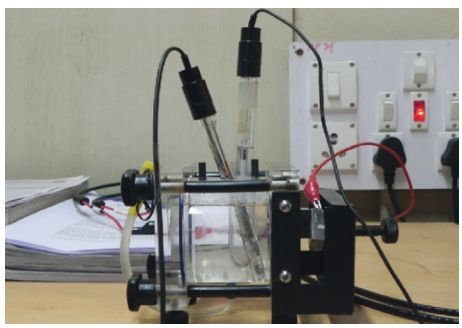

Figure 4: Polarization and impedance testing set up.

Table 4: Conditions for polarization and impedance test.

Electrolyte	3.5 wt% NaCl
Reference electrode	Saturated calomel electrode (SCH)
pH value	6–7

tested at various locations and an average was calculated [38]. The fractography analysis of different coated AZ91D Mg alloys was characterized through SEM analysis, as shown in Figures 9(d) and 9(e). Aluminum powder-coated AZ91D alloy exhibits the highest elongation with moderate strength, and fracture mode consisting of more intergranular propagation of the cracks was found [39].

Figure 10 shows the microhardness values of cast magnesium alloy, aluminum powder-coated magnesium alloy, and cathode electrodeposition (CED)-coated magnesium alloy. Among all samples, CED-coated sample showed high hardness due to good adhesion and bonding strength between substrate and coating [40]. Mg and its alloys have a low initial hardness (65–85 HV), which varies based on the strengthening phases and grain refinements. The increase in hardness on the coated alloy is mainly due to the formation of intermetallic phases and the rare-earth intermetallic combination of phases on the alloy substrate. Based on processing methods, Al powder coating hardness has been reported to range from 200 to 300 HV [27]. Vicker's indentation methods were used to investigate the mechanical characteristics of Mg-Al-Zn intermetallic phases. Al powder coating on AZ91D magnesium alloy produces the continuous $Mg_{17}Al_{12}$ and Mg_2Al_3 layers. The hardness of the $Mg_{17}Al_{12}$ and Mg_2Al_3 layers is 4.350.3 GPa and 4.400.3 GPa, respectively, which is significantly greater than the pure Mg (0.90.05 GPa) and Al powder coating on AZ91D (1.240.1 GPa) layers. The hardness of the AZ91D Mg surface shows a high value, and the hardness value gradually decreases until it reaches the hardness of the substrate matrix. The changes in microhardness value in the coating are related to the variation in composition on the substrate. Without coating AZ91D alloy and Al powder coating, CED coatings strength had been

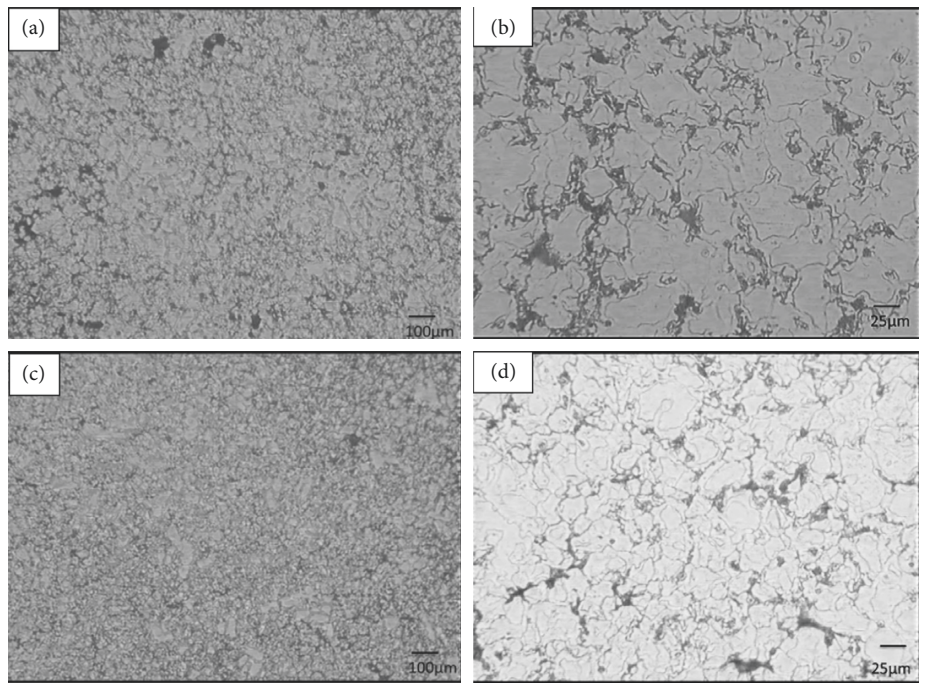

Figure 5: Optical microstructures for the CED by AZ91D+0.1wt.% Ce + 0.1wt.% Li alloy (a, b). Power coated on AZ91D+0.1wt.% Ce+0.1wt.% Li alloy (c, d).

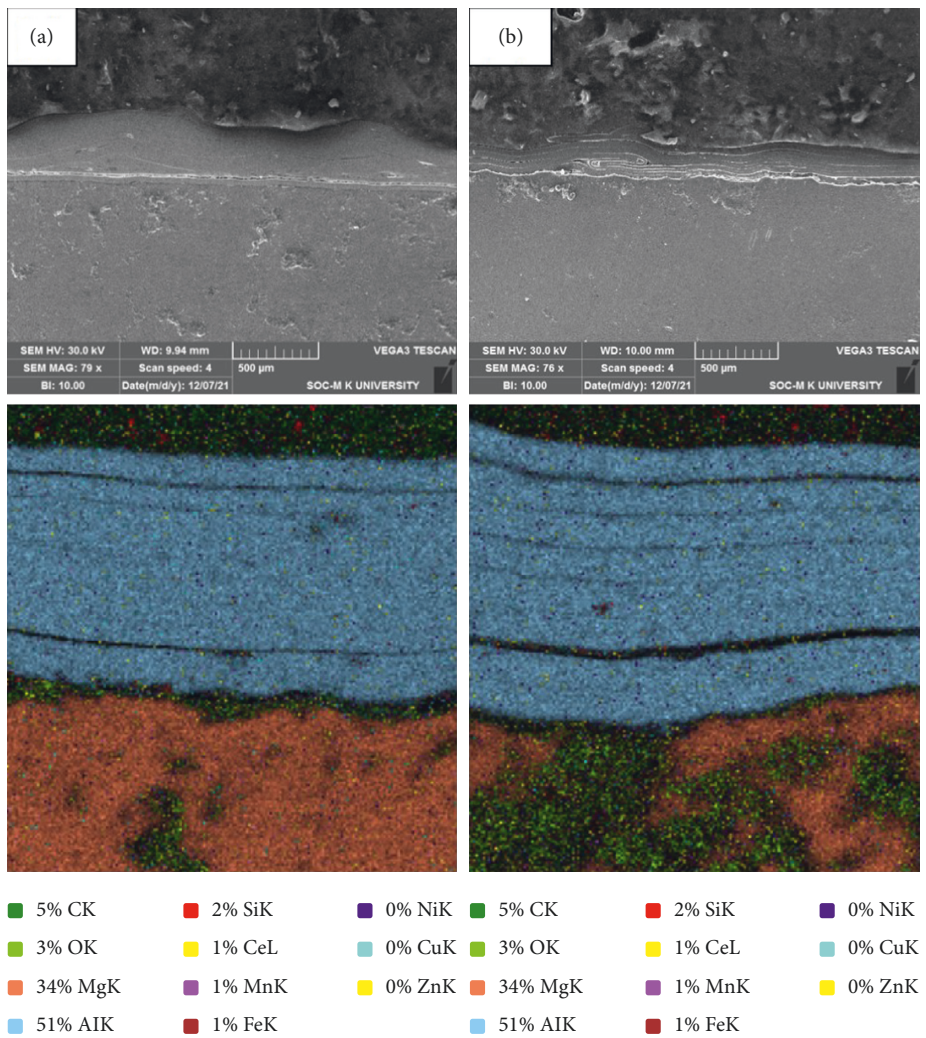

Figure 6: Cross-section micrograph for (a) Al powder coating and (b) epoxy coating on AZ91D+0.1wt.% Ce+0.1wt.% Li Mg alloy.

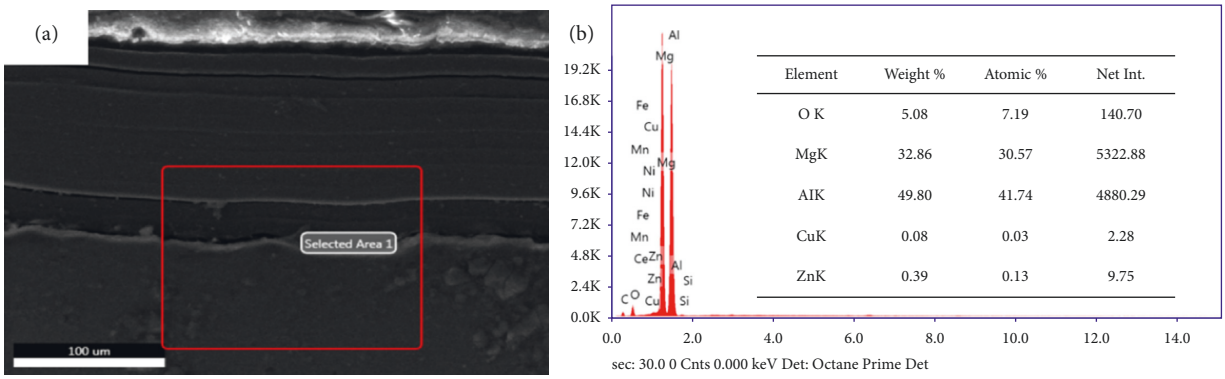

Element	Weight %	Atomic %	Net Int.
O K	5.08	7.19	140.70
MgK	32.86	30.57	5322.88
AlK	49.80	41.74	4880.29
CuK	0.08	0.03	2.28
ZnK	0.39	0.13	9.75

Figure 7: SEM images of epoxy CED samples of AZ91D+0.1wt.% Ce+0.1wt.% Li Mg alloy.

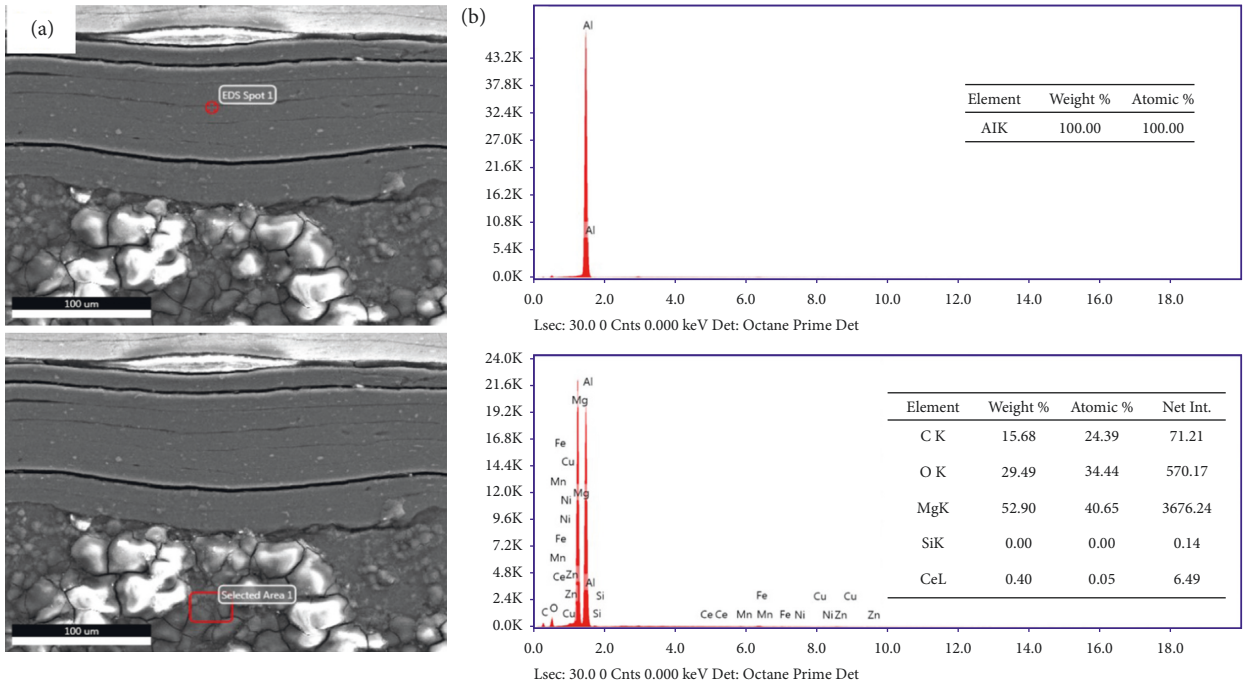

Element	Weight %	Atomic %
AlK	100.00	100.00

Element	Weight %	Atomic %	Net Int.
C K	15.68	24.39	71.21
O K	29.49	34.44	570.17
MgK	52.90	40.65	3676.24
SiK	0.00	0.00	0.14
CeL	0.40	0.05	6.49

Figure 8: SEM images of Al powder-coated samples of AZ91D+0.1wt.% Ce+0.1wt.% Li Mg alloy.

understood by tensile testing following ASTM E8 standards shown in Figure 9. The Al-enriched diffusion coating may significantly strengthen the AZ91D Mg alloys due to its high strength.

4.3. Salt Spraying Test Interpretation. The above analysis clearly states that CED-coated AZ91D shows good corrosion resistance compared to aluminum powder-coated and cast AZ91D alloys. Figure 11 shows the samples before the salt spray test, after 24 hours, and after 120 hours of the salt spray test. The specimens were taken out from the salt spray chamber, and all specimens were cleaned with acetone and then dematerialized in water, and then the samples were dried in compressed air. In the final step, chromate acid was used to immerse the samples. Corrosion products formed in the specimens were completely removed by chromate acid. The initial sample weight is measured in weighing balance (Mettler Toledo ME204) which is presented in Table 5. Then, final specimen weights were measured and mentioned in Table 6, and then corrosion rate was calculated, which is presented in Table 7. In the corrosion experiment, the corrosion rate was measured. The microscopic technique was performed on the corroded specimens.

4.4. Immersion Test Results. Table 8 shows the weight of samples before the immersion test. Figure 12 shows samples before immersion test. The sample initial weight is measured in weighing balance (Mettler Toledo ME204) which is presented in Table 9. Then, specimen final weights were measured after 24 h intervals in accordance with ASTM G31-72, and then corrosion rate is calculated which is presented in Table 10. Samples after immersion tests of 24 h, 72 h, 96 h, and 120 h are shown in Figure 13. In the immersion test experiment, the corrosion rate was found lower (45.87 mm/y) in as-cast samples when compared to CED (1.65 mm/y) and Al powder-coated samples (4.01 mm/y),

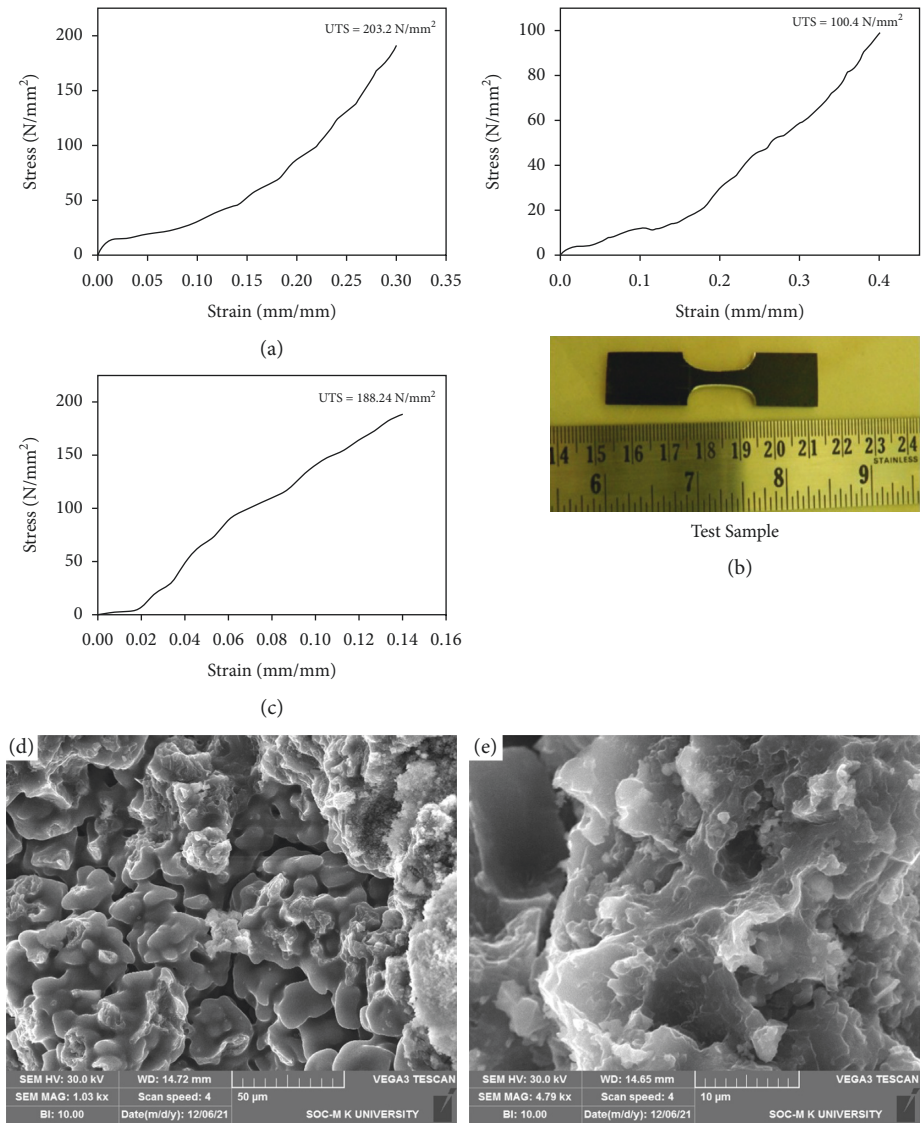

Figure 9: Tensile properties of (a) Mg CED coated, (b) Al powder coating, and (c) as cast AZ91D, and (d) fracture mode Al powder coating and (e) Fracture mode CED by epoxy.

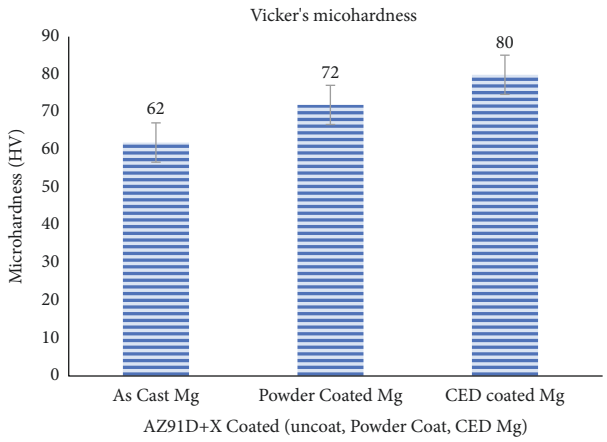

Figure 10: Vickers microhardness values.

respectively. Subsequently, compared to aluminum powder coated and cast AZ91D magnesium alloys, the data above clearly reveal that CED-coated AZ91D magnesium alloy has good corrosion resistance and the least weight loss in a 3.5% NaCl environment.

4.5. Potential-Dynamic Polarization Test and Impedance Test. The polarization curves for the different coated and uncoated samples are shown in Figure 14, and the impedance spectrum is shown in Figure 15. The electrochemical test was examined in a 3.5wt.% NaCl solution as an electrolyte, the cell with a 3-electrode cell setup (see Figure 4). M/s. ACM Gill2 instruments, India, provided this electrochemical setup. The three-electrode cell design incorporates a saturated calomel reference electrode, platinum foil-1020 mm counterelectrode, and test specimen as a working electrode (specimen). The electrolyte in the electrolytic cell is 3.5% NaCl solution, and the exposed surface area of the specimen

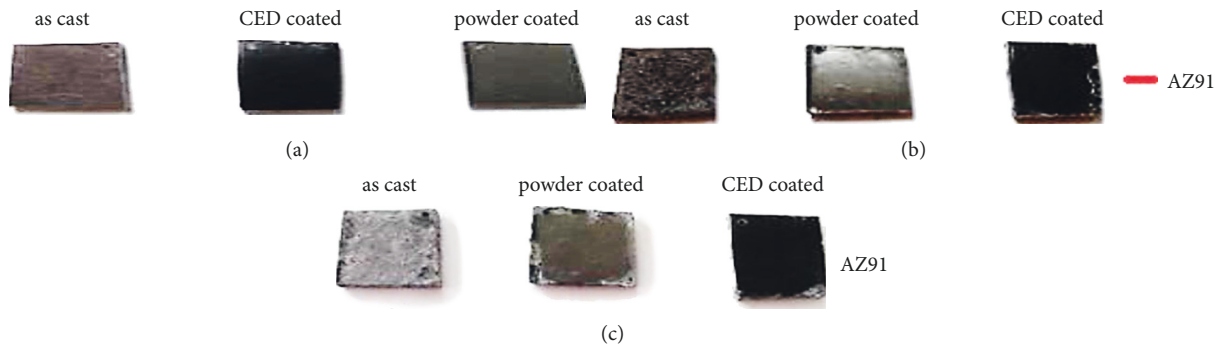

Figure 11: Salt spray test samples: (a) before the test, (b) 24 h, and (c) 120 h.

Table 5: Weight of samples before salt spray test.

Experimental alloys	Weight before the test (g)
Cast sample	3.6085 grams
Powder-coated sample	3.9256 grams
CED-coated sample	3.6356 grams

Table 6: Weight reduction of samples after 24 h, 48 h, 72 h, 96 h, and 120 h.

AZ91D	Weight after 24 h (g)	Weight after 48 h (g)	Weight after 72 h (g)	Weight after 96 h (g)	Weight after 120 h (g)
As cast sample	3.5926	3.4738	3.3679	3.2742	3.1763
Powder-coated sample	3.9163	3.9072	3.8923	3.8861	3.8732
CED-coated sample	3.6323	3.6301	3.6274	3.6244	3.6215

Table 7: Corrosion rate of AZ91D samples.

AZ91D	24 h (mm/year)	48 h (mm/year)	72 h (mm/year)	96 h (mm/year)	120 h (mm/year)
As cast sample	38.67	43.29	43.10	42.17	42.31
Powder-coated sample	3.75	3.71	4.47	3.98	4.22
CED-coated sample	1.33	1.19	1.10	1.12	1.13

Table 8: Weight of samples before immersion test.

Material	AZ91
Cast sample	3.3706 grams
Powder-coated sample	4.1533 grams
CED-coated sample	4.1083 grams

Figure 12: Samples before immersion test.

is 1 cm^2. The polarization started at a potential of around -2000 mV about the corrosion potential and terminated at a positive potential of 50 mV. The scanning rate was maintained at 10 mV/min. Cathodic polarization happens instantaneously when the magnesium electrode (specimen) is immersed in electrolyte because magnesium is too active in 3.5% NaCl solution. This experiment can be used to describe the corrosion mechanism by plotting potential and current. In the electrochemical impedance spectroscopy (EIS) test, the electrolyte and electrode are the same as in the PDP test. The frequency range measured was 1 mHz to 1 kHz, and the applied AC signal had a 5 mV amplitude. The apparent alterations in the plot imposed by coating on the polarization curve of AZ91D magnesium alloy are pushed to greater positive potentials than the AZ91D base alloy. The curve on the CED-coated sample side exhibits a stronger cathodic reaction than the base alloy. Increased cathodic reaction rates result in larger i_{corr} and E_{corr} values, as shown by Tafel charting. Table 11 shows the corresponding E_{corr} vs i_{corr} values. The CED coating significantly improves the corrosion resistance of the AZ91D magnesium alloy. According to the curve, this alloy's localized corrosion (pitting corrosion) occurred when the potential was somewhat higher than the specimen's corrosion potential in 3.5 wt % NaCl solution. The potential is begun at cathodic potential and steadily increases by 5 mV during the PDP test, resulting in a dramatic drop in corrosion current followed by anodic current near the corrosion potential, as shown in Figure 14.

Table 9: Weight reduction of samples after 24, 48, 72, 96, and 120 hours.

AZ91D	Weight after 24 h (g)	Weight after 48 h (g)	Weight after 72 h (g)	Weight after 96 h (g)	Weight after 120 h (g)
As cast sample	3.2512	3.1338	3.0283	2.9176	2.8267
Powder-coated sample	4.1421	4.1334	4.1229	4.1141	4.1036
CED-coated sample	4.1041	4.1002	4.0963	4.0925	4.0878

Table 10: Corrosion rate of samples after 24, 48, 72, 96, and 120 hours.

AZ91D	24 h (mm/year)	48 h (mm/year)	72 h (mm/year)	96 h (mm/year)	120 h (mm/year)
As cast sample	48.15	47.75	46.01	45.67	45.87
Powder-coated sample	4.51	4.02	4.08	3.98	4.01
CED-coated sample	1.69	1.63	1.61	1.61	1.65

Figure 13: Samples after immersion test of 24 h, 72 h, 96 h, and 120 h.

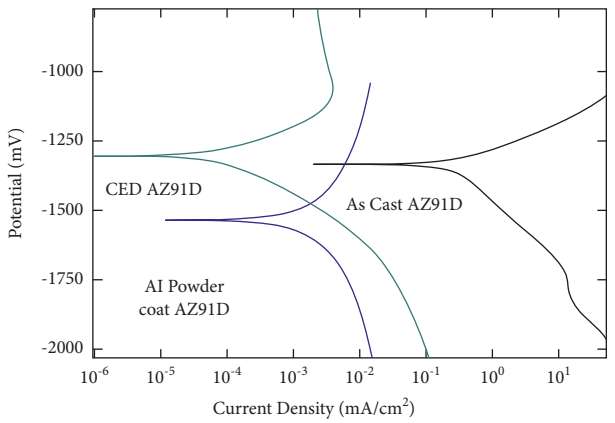

Figure 14: Variation of current density with applied voltage for AZ91 samples.

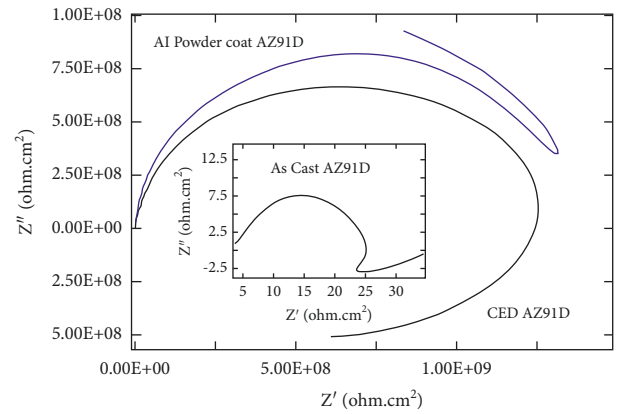

Figure 15: Impedance curves for AZ91D alloy samples.

The above electrochemical analysis clearly shows that CED-coated AZ91D magnesium alloy shows lower current density values with applied voltage and good corrosion resistance in a 3.5% NaCl environment compared to aluminum powder-coated and cast AZ91 magnesium alloys. Figure 15 represents the evolution of the impedance spectra of cast AZ91D alloy, Al powder coating on AZ91D alloy, and

Table 11: E_{corr} and I_{corr} values of AZ91 samples.

AZ91D	E_{corr} (mV)	I_{corr} (mA/cm^2)
As cast sample	−1328.7	0.0097
Powder-coated sample	−1537	7.69×10^{-4}
CED-coated sample	−1309.9	1.625×10^{-5}

epoxy coating on AZ91D alloy, respectively. Due to the creation of a passive coating on the surface of the CED AZ91D Mg alloy, the impedance magnitude (|z|) increases with time, from 2 to 10 hours. The impedance magnitude (|Z|) drops as the passive film deteriorates. In this investigation, the CED AZ91D Mg alloy was an effective barrier, preventing chlorine ions from penetrating and increasing corrosion resistance. As seen in the pitting process, when α-Mg granules corrode, precipitates form in the top layer and dissolve. As a result, the number of active atoms on the surface will rise, speeding up the formation of the protective layer. The electrochemical principle of passive and the breakdown of the passive film are demonstrated in Figure 15.

5. Conclusions

The following conclusions have been made from the above analysis. The salt spray test was completed in line with ASTM B117 standards, and the results confirmed that the immersion test was completed successfully. Impedance and potential-dynamic polarization tests were satisfactorily completed. According to the findings, CED epoxy coatings had better adhesive characteristics and corrosion resistance than powder-coated aluminum and cast magnesium. The findings show that CED epoxy coating can withstand the harsh corrosive environment found in automotive components. Compared to cast magnesium alloy, the hardness of the CED coating has increased dramatically from 71 VHN to 115 VHN. CED-coated magnesium alloy has a higher corrosion resistance than Al powder-coated magnesium alloy and casts magnesium alloy. The bonding strength of CED coating with the substrate is good compared to powder coating [41].

Data Availability

The data used to support the findings of this study are included in the article. Should further data or information be required, these are available from the corresponding author upon request.

Conflicts of Interest

The authors declare that there are no conflicts of interest regarding the publication of this paper.

Acknowledgments

The authors thank Karpagam Academy of Higher Education, Coimbatore, and Saveetha School of Engineering, SIMATS, Chennai for the technical assistance. The authors appreciate the support from Ambo University, Ethiopia.

References

[1] K. W. Guo, "A review of magnesium/magnesium alloys corrosion and its protection," *Recent Patents on Corrosion Science*, vol. 2, 2010.

[2] R. C. Zeng, E. H. Han, and W. Ke, "Corrosion of artificial aged magnesium alloy AZ80 in 3.5 wt.% NaCl solution," *Journal of Materials Science and Technology*, vol. 23, no. 3, p. 363, 2007.

[3] H. J. Martin, M. F. Horstemeyer, and P. T. Wang, "Comparison of corrosion pitting under immersion and salt-spray environments on an as-cast AE44 magnesium alloy," *Corrosion Science*, vol. 52, no. 11, pp. 3624–3638, 2010.

[4] B. L. Mordike and T. ü Ebert, "Magnesium: properties—applications—potential," *Materials Science and Engineering: A*, vol. 302, pp. 37–45, 2001.

[5] K. N. Braszczyńska-Malik, "Types of component interfaces in metal matrix composites on the example of magnesium matrix composites," *Materials*, vol. 14, p. 5182, 2021.

[6] K. N. Braszczyńska-Malik, *Precipitates of R–Mg17Al12 Phase in AZ91 Alloy*, Intechopen, London, UK, 2011.

[7] L. J. Liu and M. Schlesinger, "Corrosion of magnesium and its alloys," *Corrosion Science*, vol. 51, no. 8, pp. 1733–1737, 2009.

[8] G. J. Simandl, Hagen Schultes, S. Jana, and S. Paradis, "Magnesium-Raw materials, metal extraction and economics-global picture," in *Digging Deeper, Proceedings of the Ninth Biennial SGA Meeting*, pp. 827–831, Irish Association for Economic Geology, Dublin, UK, 2007.

[9] T. Zhu and W. Gao, "Formation of intermetallic compound coating on magnesium AZ91 cast alloy IOP Conference Series: materials Science and Engineering," *IOP Conference Series: Materials Science and Engineering*, vol. 4, no. 1, Article ID 012024, 2009.

[10] A. Bag and W. Zhou, "Tensile and fatigue behavior of AZ91D magnesium alloy," *Journal of Materials Science Letters*, vol. 20, no. 5, pp. 457–459, 2001.

[11] M. K. Kulekci, "Magnesium and its alloys applications in automotive industry," *International Journal of Advanced Manufacturing Technology*, vol. 39, no. 9-10, pp. 851–865, 2008.

[12] S. Mathieu, C. Rapin, J. Steinmetz, and P. Steinmetz, "A corrosion study of the main constituent phases of AZ91 magnesium alloys," *Corrosion Science*, vol. 45, no. 12, pp. 2741–2755, 2003.

[13] A. A. Luo, "Magnesium: current and potential automotive applications," *Jom*, vol. 54, no. 2, pp. 42–48, 2002.

[14] J. El Gray and B. Luan, "Protective coatings on magnesium and its alloys—a critical review," *Journal of Alloys and Compounds*, vol. 336, no. 1-2, pp. 88–113, 2002.

[15] W. Wulandari, G. Brooks, M. Rhamdhani, and B. Monaghan, "Magnesium: current and alternative production routes," in *Proceedings of the Australasian Conference on Chemical Engineering Barton, A.C.T., Engineers Australia, Adelaide*, SA, Australia, September 2010.

[16] R. Ambat, N. N. Aung, and W. Zhou, "Evaluation of microstructural effects on corrosion behaviour of AZ91D magnesium alloy," *Corrosion Science*, vol. 42, no. 8, pp. 1433–1455, 2000.

[17] C. Zhong, F. Liu, Y. Wu et al., "Protective diffusion coatings on magnesium alloys: a review of recent developments," *Journal of Alloys and Compounds*, vol. 520, pp. 11–21, 2012.

[18] D.-C. Chen, J.-F. Wu, Yi-Q. Liang, S.-L. Ye, and W.-F. Li, "Preparation of cerium oxide based environment-friendly chemical conversion coating on magnesium alloy with additives," *Transactions of Nonferrous Metals Society of China*, vol. 21, no. 8, pp. 1905–1910, 2011.

[19] Y.-F. Jiang, H.-T. Zhou, and Su-M. Zeng, "Microstructure and properties of oxalate conversion coating on AZ91D magnesium alloy," *Transactions of Nonferrous Metals Society of China*, vol. 19, no. 6, pp. 1416–1422, 2009.

[20] Z. Yang, J. P. Li, J. X. Zhang, G. W. Lorimer, and J. A. M. S. E. L. Robson, "Review on research and development of magnesium alloys," *Acta Metallurgica Sinica*, vol. 21, no. 5, pp. 313–328, 2008.

[21] H. Altun and S. Sen, "The effect of PVD coatings on the corrosion behaviour of AZ91 magnesium alloy," *Materials and Design*, vol. 27, no. 10, pp. 1174–1179, 2006.

[22] Z. Li, Q. Ren, X. Wang et al., "Effect of phosphate additive on the morphology and anti-corrosion performance of plasma electrolytic oxidation coatings on magnesium—lithium alloy," *Corrosion Science*, vol. 157, pp. 295–304, 2019.

[23] V. K. Korrapati, N. Scharnagl, D. Letzig, and M. L. Zheludkevich, "Bilayer coatings for temporary and long–term corrosion protection of magnesium–AZ31 alloy," *Progress in Organic Coatings*, vol. 163, Article ID 106608, 2022.

[24] S.-J. Lee and L. H. T. Do, "Effects of copper additive on micro-arc oxidation coating of LZ91 magnesium-lithium alloy," *Surface and Coatings Technology*, vol. 307, pp. 781–789, 2016.

[25] S.-Yi Jian, Yu-C. Tzeng, M. D. Ger et al., "The study of corrosion behavior of manganese-based conversion coating on LZ91 magnesium alloy: effect of addition of pyrophosphate and cerium," *Materials & Design*, vol. 192, Article ID 108707, 2020.

[26] X. c Ma, S. y Jin, R. z Wu et al., "Corrosion behavior of Mg– Li alloys: a review," *Transactions of Nonferrous Metals Society of China*, vol. 31, pp. 3228–3254, 2021.

[27] C. Zhong, M. F. He, L. Liu et al., "Formation of an aluminum-alloyed coating on AZ91D magnesium alloy in molten salts at lower temperature," *Surface and Coatings Technology*, vol. 205, pp. 2412–2418, 2010.

[28] K. Hemalatha, C. James, L. Natrayan, and V. Swamynadh, "Analysis of RCC T-beam and prestressed concrete box girder bridges super structure under different span conditions," *Materials Today Proceedings*, vol. 37, pp. 1507–1516, 2021.

[29] G. Choubey, Y. Devarajan, W. Huang, L. Yan, H. Babazadeh, and K. Pandey, "Hydrogen fuel in scramjet engines - a brief review," *International Journal of Hydrogen Energy*, vol. 45, no. 33, pp. 16799–16815, 2020.

[30] V. Balaji, S. Kaliappan, D. M. Madhuvanesan et al., "Combustion analysis of biodiesel-powered propeller engine for least environmental concerns in aviation industry," *Aircraft Engineering & Aerospace Technology*, vol. 94, no. 5, pp. 760–769, 2022.

[31] D. Veeman, M. S. Sai, P. Sureshkumar et al., "Additive manufacturing of biopolymers for tissue engineering and regenerative medicine: an overview, potential applications, advancements, and trends," *International Journal of Polymer Science*, vol. 202120 pages, Article ID 4907027, 2021.

[32] S. Justin Abraham Baby, S. Suresh Babu, and Y. Devarajan, "Performance study of neat biodiesel-gas fuelled diesel engine," *International Journal of Ambient Energy*, vol. 42, no. 3, pp. 269–273, 2018.

[33] K. Seeniappan, B. Venkatesan, N. N. Krishnan et al., "A comparative assessment of performance and emission characteristics of a DI diesel engine fuelled with ternary blends of two higher alcohols with lemongrass oil biodiesel and diesel fuel," *Energy & Environment*, vol. 13, p. 0958305X2110513, 2021.

[34] V. S. Nadh, C. Krishna, L. Natrayan et al., "Structural behavior of nanocoated oil palm shell as coarse aggregate in lightweight concrete," *Journal of Nanomaterials*, vol. 20217 pages, Article ID 4741296, 2021.

[35] Y. Devarajan, G. Choubey, and K. Mehar, "Ignition analysis on neat alcohols and biodiesel blends propelled research compression ignition engine," *Energy Sources, Part A: Recovery, Utilization, and Environmental Effects*, vol. 42, no. 23, pp. 2911–2922, 2019.

[36] S. Kaliappan, M. D. Raj Kamal, S. Mohanamurugan, and P. K. Nagarajan, "Analysis of an innovative connecting rod by using finite element method," *Taga Journal Of Graphic Technology*, vol. 14, pp. 1147–1152, 2018.

[37] L. Natrayan and A. Merneedi, "Experimental investigation on wear behaviour of bio-waste reinforced fusion fiber composite laminate under various conditions," *Materials Today Proceedings*, vol. 37, pp. 1486–1490, 2021.

[38] Y. Devarajan, B. Nagappan, G. Choubey, S. Vellaiyan, and K. Mehar, "Renewable pathway and twin fueling approach on ignition analysis of a dual-fuelled compression ignition engine," *Energy and Fuels*, vol. 35, no. 12, pp. 9930–9936, 2021.

[39] A. S. Kaliappan, S. Mohanamurugan and P. K. Nagarajan, "Numerical investigation of sinusoidal and trapezoidal piston profiles for an IC engine," *Journal of Applied Fluid Mechanics*, vol. 13, no. 1, pp. 287–298, 2020.

[40] R. Venkatesh, S. Manivannan, S. Kaliappan et al., "Influence of different frequency pulse on weld bead phase ratio in gas tungsten arc welding by ferritic stainless steel AISI-409L," *Journal of Nanomaterials*, vol. 2022, Article ID 9530499, 11 pages, 2022.